Efficient prediction methods for the micro-pressure wave from a high-speed train entering a tunnel using the Kirchhoff formulation

Taeseok Yoon
Department of Aerospace Engineering, Seoul National University, BD 136-318, Seoul National University, Seoul 151-742, Korea

Soogab Lee[a)]
IAAT (Institute of Advanced Aerospace Technology), School of Mechanical and Aerospace Engineering, Seoul National University, BD 301-1303, Seoul National University, Seoul 151-742, Korea

(Received 18 March 2001; accepted for publication 13 August 2001)

The compression wave generated by a high-speed train emerging from the exit portal of a tunnel gives rise to an impulsive noise called a micro-pressure wave. In this study, new methods for the prediction of sonic-boom noise are proposed. The first method combines acoustic monopole analysis and the method of characteristics with the Kirchhoff method. The compression wave from a train entering a tunnel is calculated by an approximate compact Green's function, and the resultant noise at the tunnel exit is predicted by a linear Kirchhoff formulation. The second method couples the Kirchhoff formulation with the Euler equation, which is solved numerically for the generation and propagation of the compression wave. Numerical prediction of the compression wave, the propagation in the tunnel, and the micro-pressure wave obtained by the present methods are compared with measured data. The numerical results exhibit a reasonable agreement with the experimental data. The proposed methods in this study are shown to be very useful design tools for the nose shape of trains and the geometry of tunnels, and they can be utilized to minimize the pressure fluctuation in the tunnel and the corresponding booming noise. [DOI: 10.1121/1.1409374]

PACS numbers: 43.50.Lj, 43.50.Pn, 43.28.Ra [MRS]

NOMENCLATURE

a_∞	speed of sound
a	height of tunnel
A	uniform cross-sectional area of tunnel
A_0	uniform cross-sectional area of train
A_T	variable cross-sectional area of train
b,D	width of tunnel ($=2b'$)
e	total energy per unit volume
$h_{\max}$	maximum train height
L	length of tunnel
l_p	length of profiled nose
l'	end-correction
M	train Mach number ($=U/a_\infty$)
$\mathbf{n}$	normal vector on the surface
p'	acoustic pressure
q	strength of volume source
Q	source strength
r	distance between a source position at the sound generation time and an observer at the sound receiving time
t	observer time
Δt	computational time step
U	speed of train
u,v,w	velocity components in x, y, z direction
x_p	measured or predicted position of pressure fluctuation in the tunnel
x, y, z	Cartesian coorinates
γ	ratio of specific heat
ϕ	velocity potential
ϕ^*	potential function
ρ_0	mean air density
ρ	density
θ	angle between the normal vector on the surface and the radiation vector
τ	retarded time ($=[t]$)
Ω	solid angle representing the configuration around the tunnel exit

I. INTRODUCTION

When a high-speed train enters a tunnel, a compression wave is generated ahead of the train, which propagates along the tunnel. The parameters affecting the magnitude and the gradient of the compression waves are train speed, blockage ratio, nose shape, etc. When the wave front of the compression wave arrives at the exit of the tunnel, a pressure pulse is radiated out, causing a strong impulsive noise, which becomes a serious environmental problem. This pressure pulse (or ''micro-pressure wave'') often results in structural damage of the tunnel and much annoyance for the population near the exit. The strength of the micro-pressure wave is

[a)]Electronic mail: solee@plaza.snu.ac.kr

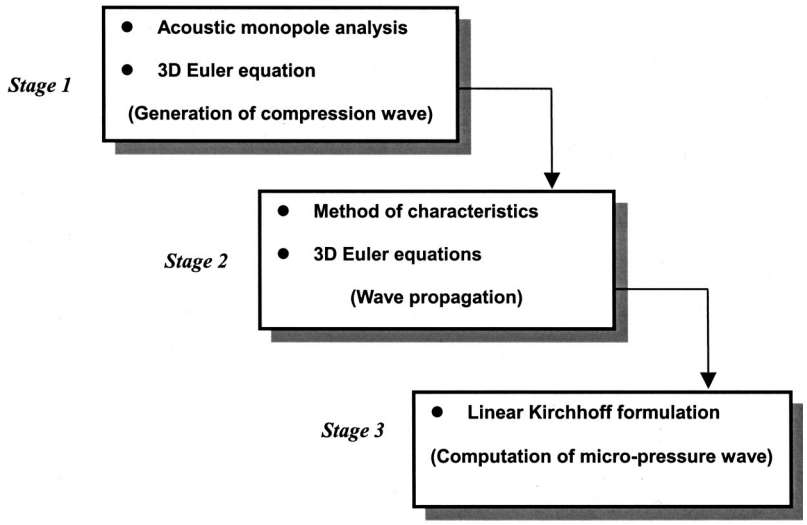

FIG. 1. Schematic of the prediction procedure for the micro-pressure wave (combined acoustic monopole analysis/method of characteristics–Kirchhoff method and CFD–Kirchhoff method).

proportional to the gradient of the incident compression wave. If a tunnel with a concrete slab track is longer than 3 km, a nonlinear steepening of the compression wave can produce a micro-pressure wave with peak magnitudes of over 50 Pa. The peak value of the micro-pressure wave depends on the train speed, the cross-sectional area ratio of train to tunnel, the train nose shape, and so on.[1]

The wave physics related to the micro-pressure wave can be divided into three phases:

(1) generation of the compression wave by a train entering a tunnel,
(2) propagation of the compression wave in tunnel, and
(3) emission of a micro-pressure wave at the tunnel exit.

In the current work, the formation of the compression wave is predicted by an empirical formula,[1] which uses parameters such as the train speed and the blockage ratio. The nose shape of the train, which plays an important role in formation of the compression wave, however, is not considered in the empirical formula. A sufficiently slender nose profile can reduce the micro-pressure wave strength by about 3 dB.[2,3] Therefore, the empirical formula from Ref. 1 in its original form is not adequate for the design procedure of train and tunnel. Howe analyzed the compression wave by using the exact acoustic Green's function for a semi-infinite and circular-cylindrical tunnel. He treated the nose of the train by a distribution of monopole sources along its symmetric axis, and calculated their interaction with the mouth of the tunnel.[4] He also derived the analytical representations of the Green's function describing the generation of sound waves within a semi-infinite flanged cylinder with sources located in the neighborhood of an open end using Rayleigh's method for the approximate calculation of out-going potential flow.[5,6] His approach was demonstrated for the flanged and cylindrical tunnels of semi-circular and rectangular cross sections, where exact analytic solutions of potential functions are not available. This analytical method can also consider arbitrary shapes of tunnels. As for the numerical approach to predict the compression wave, two- and three-dimensional Euler/Navier–Stokes solvers are used. Many approaches considering the effect of nose shape have attempted to analyze only the compression wave at the entrance of the tunnel.[7–9] Compared to other methods, this numerical approach requires much computational cost and time.

At stage (2), the propagation of the compression wave can be simulated by the method of characteristics using a one-dimensional Euler equation[10,11] or two/three-dimensional Euler/Navier–Stokes solvers. Only the case of a short tunnel (about 1 km) is adequate for two/three-dimensional Euler/Navier–Stokes calculations, considering the restriction of computer memory and time consumption.

For the prediction of the micro-pressure wave, the relationship between two waves (the micro-pressure wave and the compression wave) has been derived using the acoustic model of a vibrating circular piston on an infinite baffle plate.[1,12,13] Yoon *et al.* proposed a new method for the sonic boom noise using a linear Kirchhoff formulation which requires no approximation of frequency range. Furthermore, the method has an additional advantage in that it can predict the directivity of the micro-pressure wave.[14]

In this article, new methods to predict the micro-pressure wave are proposed. First, a CFD (computational fluid dynamics) technique is combined with a Kirchhoff formulation. An Euler finite difference solver is first executed to solve the near field. The resulting data are then transferred to the linear Kirchhoff formulation to predict the far field acoustics. The process is named the combined CFD–Kirchhoff method. The second method combines Howe's theory for the formation of the compression wave and the method of characteristics for the propagation of the compression wave with the Kirchhoff formulation. The method is named combined acoustic monopole analysis/method of characteristics–Kirchhoff formulation. Figure 1 summarizes the schematic of the above numerical and analytic calculation procedures.

The prediction results of the proposed methods are compared with each other and are validated with experimental data obtained in the Train Test Facility (T3F) at National Aerospace Laboratory (NLR) in the Netherlands.[14] Axisymmetric model trains and a tunnel of rectangular cross section

are used for the prediction and validation of the compression wave and the micro-pressure wave. The blockage ratio and other specifications will be discussed in Sec. V.

The present study is aimed at developing a useful design tool for the nose shape of high-speed trains and tunnel cross sections that can minimize the discomfort of passengers and mitigate the micro-pressure wave. The significance of the study reaches beyond just engineering interest in that the complex physical phenomena of aeroacoustics and aerodynamics are studied.

II. ACOUSTIC MONOPOLE ANALYSIS AND METHOD OF CHARACTERISTICS

A. Acoustic monopole analysis for formation of a compression wave

The velocity potential $\phi(\mathbf{x},t)$ of the sound generated by a distribution of volume source $q(\mathbf{x},t)$ is governed by the inhomogeneous wave equation

$$\frac{1}{a_\infty^2}\frac{\partial^2\phi(\mathbf{x},t)}{\partial t^2}-\frac{\partial^2\phi(\mathbf{x},t)}{\partial x^2}=-q(\mathbf{x},t). \tag{1}$$

The tunnel walls and surfaces of adjacent solid structures are assumed to be sufficiently rigid that the potential satisfies the wall boundary condition $\partial\phi/\partial x_n=0$ on all surfaces. The solution to Eq. (1) takes on the following form:

$$\phi(\mathbf{x},t)=-\int\int_V G(\mathbf{x},\mathbf{y};t-\tau)q(\mathbf{y},\tau)\,d^3\mathbf{y}d\tau. \tag{2}$$

Here, Green's function $G(\mathbf{x},\mathbf{y};t-\tau)$ is the solution of Eq. (1) if the right-hand side is replaced by the impulsive point source $\delta(\mathbf{x}-\mathbf{y})\delta(t-\tau)$. The integration in Eq. (2) is over the whole region of the fluid and over the time τ. Function G should satisfy both $\partial G/\partial x_n=0$ and $\partial G/\partial y_n=0$, where the field points $\mathbf{x},\mathbf{y}$ lie on the rigid tunnel boundaries and the solid surfaces outside the tunnel mouth.

When the tube is semi-infinite with an open end, the radiated sound wave resulting from the interaction of source q and the exit is determined by the following compact approximation of G:[5,6]

$$G(\mathbf{x},\mathbf{y};t-\tau)\approx\frac{a_\infty}{2A}\left\{H\left(t-\tau-\frac{|\phi^*(\mathbf{x})-\phi^*(\mathbf{y})|}{a_\infty}\right)-H\left(t-\tau+\frac{|\phi^*(\mathbf{x})+\phi^*(\mathbf{y})|}{a_\infty}\right)\right\}, \tag{3}$$

where $\phi^*(\mathbf{x})$ is the solution of Laplace's equation for incompressible and irrotational flow and $H(x)$ is the Heaviside unit step function. The function is normalized such that

$$\phi^*(\mathbf{x})\sim\begin{cases}x-\mathrm{l}' & \text{as } x\to-\infty \text{ in the tube,}\\ O(1/|\mathbf{x}|) & \text{as } x\to\infty \text{ outside the tube.}\end{cases}$$

In these equations, l' represents the "end-correction" of the tunnel mouth, which depends on the details of tunnel entrance geometry. The potential function $\phi^*(\mathbf{x})$ plays an important role in the calculation of sound generated by sources in the neighborhood of the open tunnel end provided the frequency is sufficiently small that the acoustic wave length is much larger than the tunnel diameter. Equation (3) is uniformly valid when regarded as a function of either $\mathbf{x}$ or $\mathbf{y}$, provided at least one of these points lies within the tunnel at a distance from the mouth large compared to the tunnel diameter.

The solution (3) determines the entry compression wave, prior to the propagation of wave in the tunnel, and is valid up to several tunnel diameters ahead of the train slightly after it enters the tunnel. The perturbation pressure p can be calculated from the linearized Bernoulli equation $p=-\rho_0\partial\phi/\partial t$. This yields the following form when Eq. (3) is substituted into Eq. (2):

$$p(\mathbf{x},t)=\frac{\rho_0 a_\infty}{2A}\int\{q(x'+U[t]-\mathrm{M}\phi^*(\mathbf{x}'),y',z')-q(x'+U[t]+\mathrm{M}\phi^*(\mathbf{x}'),y',z')\}\,d^3\mathbf{x}'. \tag{4}$$

Here, $[t]\approx t+(x-\mathrm{l}')/a_\infty$, and is the retarded time.

The source distribution q is nonzero only in the vicinity of the nose and tail where its cross-sectional area is changing. The compression wave is generated as the nose enters the tunnel and the length of the train should be assumed to be so large that the rear end can be ignored. If the train Mach number is so small that $O(M^2)$ and $M\phi^*(\mathbf{x}')$ terms are negligible during the formation of the compression wave, then

$$p\approx p(x,t)=\frac{\rho_0 U}{a}\int q(\mathbf{x}'+U[t],y',z')\frac{\partial\phi^*(\mathbf{x}')}{\partial x}d^3\mathbf{x}'. \tag{5}$$

Equation (5) describes the generation of a compression wave during the passage of the train nose into the tunnel. The monopole source distribution considering the nose shape of an axisymmetric train is as follows:

$$q(\mathbf{x}-\mathbf{U}t)=UA_0Q(x-Ut)\,\delta(y)\,\delta(z), \tag{6}$$

$$Q(x)=\frac{1}{A_0}\frac{\partial A_T(x)}{\partial x}. \tag{7}$$

Howe[5] suggested an extrapolation formula to extend the Mach number restriction. The prediction of Eq. (5) for very small Mach numbers can be modified to larger Mach numbers (about to 0.4) by the consideration of compressibility:

$$p(x,t)\approx\frac{\rho_0 U^2A_0}{(1-\mathrm{M}^2)A}\int Q(x'+U[t])\frac{\partial\phi^*(x',0,z_T)}{\partial x'}d\mathbf{x}'. \tag{8}$$

In Eq. (5), the Rayleigh method for estimating the length of end-correction supplies an approximate representation of $\phi^*(x)$ for arbitrary shape of a given cross-sectional area of the tunnel. The function $\phi^*(x)$ is known analytically only for an unflanged and semi-infinite circular cylinder. Approximate representations of $\phi^*(x)$ for circular flanged ducts or rectangular cross-section can be obtained by the Rayleigh method.

For a rectangular tunnel with a flanged portal of height a and width b, the potential $\phi^*(x)$ describes potential flow from the rectangular duct of cross-section $2a\times b$ obtained from removal of the ground plane and introduction of the

image of the tunnel in $y=0$. Rayleigh's method is applied by taking $u(y,z)$, the exit plane velocity in the following form:[5]

$$u(0,y,z)=\frac{\partial\phi'}{\partial x}=\alpha\left(1+\frac{\mu_a y^4}{a^4}+\frac{\mu_b z^4}{b'^4}\right). \tag{9}$$

where $\alpha=1/[1+(\mu_a+\mu_b)/5]$.

The distribution of the potential function inside the tunnel $(x<0)$ is

$$\phi^*(x)=x-l'\sum_{n=1}^{\infty}\frac{8\alpha(-1)^n}{n^3\pi^3}\left(1-\frac{6}{n^2\pi^2}\right)\times\left\{a\mu_a\cos\left(\frac{n\pi y}{a}\right)e^{n\pi x/a}+b'\mu_b\cos\left(\frac{n\pi z}{b'}\right)e^{n\pi x/b'}\right\}. \tag{10}$$

Function $\phi^*(x)$ outside the tunnel $(x>0)$ is given as follows:

$$\phi^*(x)=\frac{-1}{2\pi}\int_{S_0}\frac{u(y',z')dy'dz'}{\sqrt{x^2+(y-y')^2+(z-z')^2}}. \tag{11}$$

The coefficients of μ_a and μ_b are determined to minimize the length of end-correction by Kelvin's minimum energy principle. The value of μ_a and μ_b will be mentioned later in Sec. V.

B. Method of characteristics for propagation of compression wave

The micro-pressure wave depends on the waveform of the incident compression wave at the tunnel exit. The magnitude of the micro-pressure wave is approximately proportional to the time derivative of the pressure of the incident compression wave $(\partial p/\partial t)$. The micro-pressure wave becomes larger in a long tunnel with a concrete slab track because the wave front of the compression wave becomes steep due to a nonlinear effect during the propagation. In a long ballasted track tunnel, the wave front of the compression wave does not steepen and the pressure gradient of the wave front decreases during propagation. The maximum value of the micro-pressure wave in long ballasted track tunnels becomes smaller than that in short tunnels.[1]

The effect of a ballasted track is attributed to its porosity. A ballasted track can be regarded as a porous sound-absorbing material, which is effective in the low-frequency range. Penetration of air into the ballasted track causes a dissipation effect and prevents the wave front of the compression wave from steepening.

The hyperbolic wave equation for the forward-moving compression wave in a one-dimensional sense is as follows:

$$\frac{\partial u}{\partial t}+\left\{(1-\alpha_c)a_\infty+\frac{\gamma+1}{2}u\right\}\frac{\partial u}{\partial x}=\frac{1}{2}\left\{f_1+\nu^*\frac{\partial^2 u}{\partial x^2}\right\}, \tag{12}$$

where u is the medium air velocity accompanying the compression wave, f_1 is the frictional force at the periphery of the tunnel, γ is the specific heat ratio of air, and x is the spatial coordinate along the tunnel. The coefficients α_c $(=1.4\times10^{-3})$ and $\nu^*(=4.35\times10^{-5})$ of Eq. (12) represent the effect on propagation velocity of compression wave and the dissipation effect, respectively.[15]

III. CFD FOR FORMATION AND PROPAGATION OF COMPRESSION WAVE

A. CFD technique

An unsteady, compressible, and three-dimensional Euler equation is solved to analyze the flow field around the high-speed train. The system of equations consists of a local time derivative term and three convective flux vectors. In physical coordinates, the governing equation is

$$\frac{\partial Q}{\partial t}+\frac{\partial E}{\partial x}+\frac{\partial F}{\partial y}+\frac{\partial G}{\partial z}=0, \tag{13}$$

where

$$Q=\begin{pmatrix}\rho\\ \rho u\\ \rho v\\ \rho w\\ \rho e\end{pmatrix},\quad E=\begin{pmatrix}\rho u\\ \rho u^2+p\\ \rho uv\\ \rho uw\\ (\rho e+p)u\end{pmatrix},$$

$$F=\begin{pmatrix}\rho v\\ \rho uv\\ \rho v^2+p\\ \rho vw\\ (\rho e+p)v\end{pmatrix},\quad G=\begin{pmatrix}\rho w\\ \rho uw\\ \rho vw\\ \rho w^2+p\\ (\rho e+p)w\end{pmatrix}.$$

The equation of state is

$$e=\frac{1}{\rho(\gamma-1)}p+\frac{1}{2}(u^2+v^2+w^2). \tag{14}$$

Roe's finite volume flux difference splitting technique, based upon the solution of Riemann problem[16] is used for spatial discretization and MUSCL (monotone upstream-centered scheme conservation laws) with a van Albada flux limiter used to achieve third-order spatial accuracy. Calculations of unsteady flow field around a moving body require a time accurate numerical integration. In the present study, Yoon's LU-SGS scheme[17] is chosen for efficient time marching due to the huge demand on computer power.

B. Grid systems

The grid system for computation of the three-dimensional train/tunnel aerodynamic interaction is characterized by a moving body confined to linear motions on the rail, relative motions between the solid body and the background grid, ground proximity, and large computational domains through which a train moves.

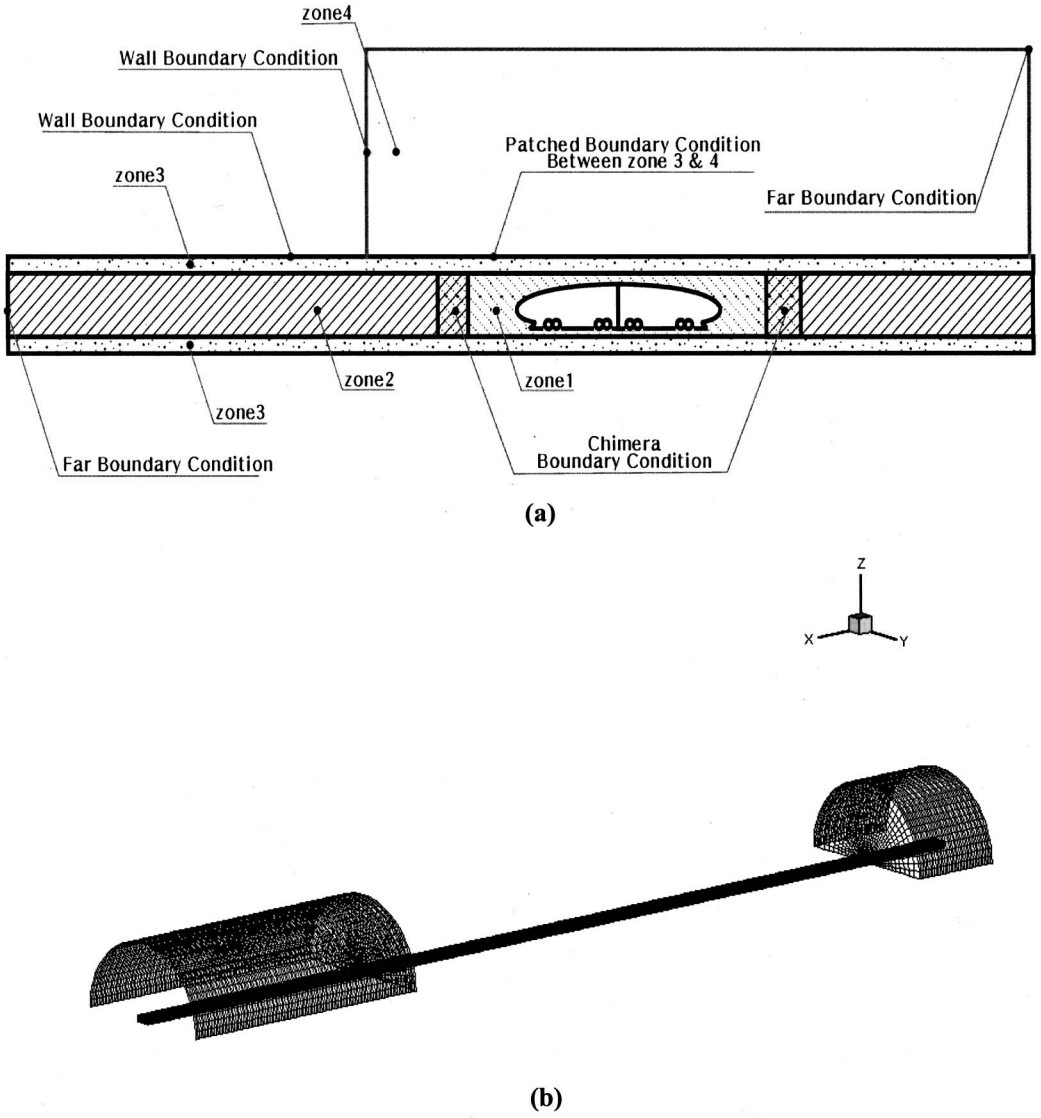

FIG. 2. (a) Schematic diagram for zone decomposition and boundary condition and (b) five-block grid system for the CFD calculation.

To accommodate the relative motion, Fujii[9,18] used FSA (fortified solution algorithm) while Mestreau[19] used an unstructured grid with automatic remeshing. Fujii's approach for the current problem is similar to the Chimera[20] procedure composed of hole construction and linear interpolation at the boundaries. To obtain a stable solution, a moderate cell volume ratio between a giving cell and a target cell has to be maintained at the boundaries. If the region swept by the train is large, a huge number of grid points along the region is required in order to preserve the proper interpolation criterion. Fujii used an intermediate zone to overcome this requirement, but this method made the linear interpolation routine more complicated. In this study, three types of DDT (domain decomposition technique) are applied. They are multi-block, patched, and overlapping grids to obtain both computational efficiency and extensibility.

TABLE I. Number of grid points used for prediction flow field.

Zone	Grid (x,y,z)	Sum of grid
1	(71,23,25)	40 825
2	(431,23,25)	247 825
3	(431,23,5)	49 565
4	(120,18,25)	54 000
5	(40,18,25)	18 000
Total sum of grid		410 215

Figure 2 shows the schematic zone decomposition and the zonal interface for this problem. Zone 1 moves with the high-speed train while zone 2 is fixed. Consequently, a simplified Chimera hole construction and linear interpolation are applied at the fore and aft overlapping regions of the moving train. As no stiff gradient of the flow variables exists except in the vicinity of the train, and as the wave phenomena in the tunnel are almost one-dimensional, linear interpolation is sufficient without adopting a tedious and complicated three-dimensional conservative treatment.[21] Zone 3 is an intermediate zone sharing a sliding surface with zone 1. Zone 4 is the tunnel entrance zone. At the tunnel exit, zone 5 similar to zone 4 can be defined. Table I lists the number of grid points used for prediction of near field flow. In the computations, a constant computational time step of $\Delta t = 0.01$/iteration is used. It takes approximately 16 s per iteration at 450 Mhz

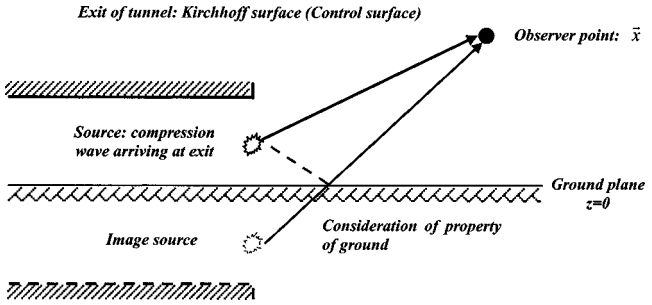

FIG. 3. Kirchhoff (control) surface for prediction of the micro-pressure wave and consideration of the effect of ground (image source of sound).

with a digital Alpha CPU. The length and time scales are normalized by D and D/a_∞, respectively, where D is the width of the tunnel.

IV. KIRCHHOFF FORMULATION FOR RADIATION OF MICRO-PRESSURE WAVE

A linear Kirchhoff formulation is applied to predict the micro-pressure wave at the tunnel exit. The near field flow data obtained by acoustic monopole analysis/method of characteristics or CFD are used as an input to Kirchhoff formulation. The Kirchhoff integral formula for a stationary control surface is the analytic expression of Huygens' principle.[22] The Kirchhoff formulation is as follows:

$$p'(\mathbf{x},t)=\frac{1}{4\pi}\int_S\int\left[\frac{\cos\theta}{r^2}p'-\frac{1}{r}\frac{\partial p'}{\partial n}+\frac{\cos\theta}{a_\infty r}\frac{\partial p'}{\partial \tau}\right]dS(\mathbf{y},\tau). \quad (15)$$

Here, p' is the perturbed pressure, ($\mathbf{x}$, t) are the observer's location and time, ($\mathbf{y}$, τ) are the source location and retarded time variables, θ is the angle between the normal vector ($\mathbf{n}$) on the surface and the radiation vector ($\mathbf{r}$), and r is the distance between an observer and a source at the retarded time. Note that pressure and its derivatives are calculated at the retarded time, τ. Equation (15) has been widely used for aeroacoustic predictions of high-speed impulsive noise and transonic blade-vortex interaction noise generated by a rotor.[23–25]

The integration is performed at the control surface, called the Kirchhoff surface, containing the flow field information. In the present study, the exit plane normal to the tunnel exit is considered as the control surface, and the image source of sound is imposed to consider the ground effect. The coefficient of sound absorption varies with the frequency of the incident wave and the material property.[26] Us-

TABLE II. Test types used in prediction and validation.

Test type	Model train (mm^2)	Tunnel area (mm^2)	Blockage ratio (%)	Aspect ratio (h_{max}/l_p)
A (K-TGV)	314.2	3680	8.5	10 mm/40 mm
B (Short nose)	314.2	3880	8.1	10 mm/40 mm
C (Long nose)	314.2	3880	8.1	10 mm/70 mm

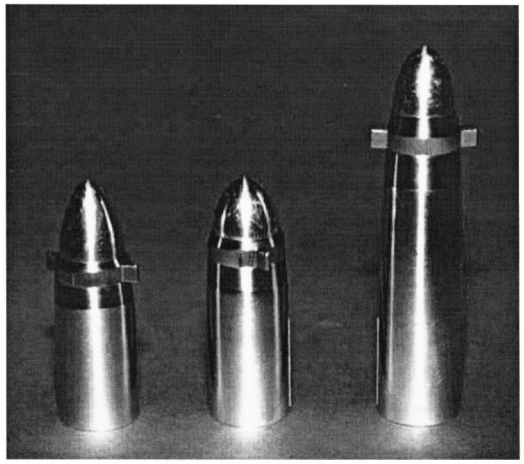

(a)

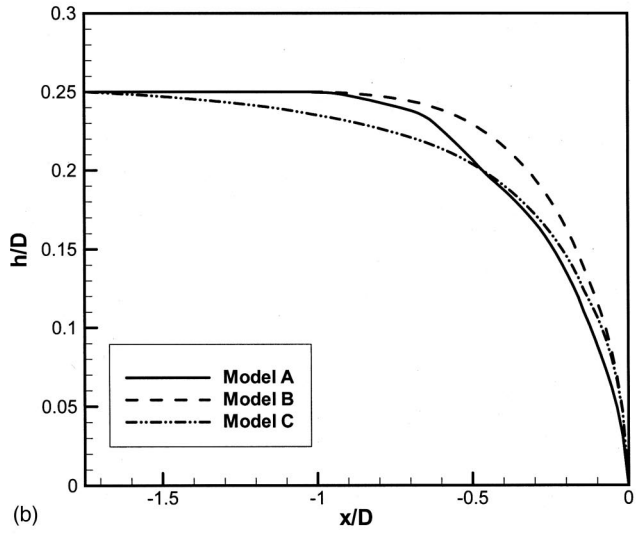

(b)

FIG. 4. (a) Axisymmetric model trains A, B, and C and (b) a sketch of the model train.

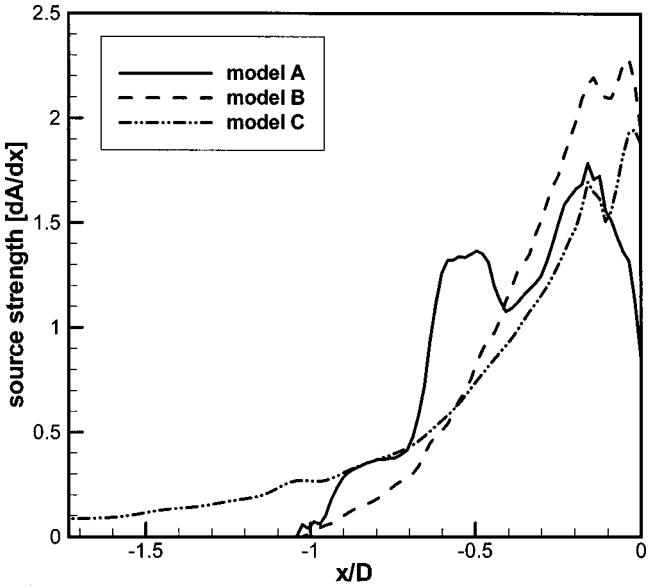

FIG. 5. Source strength of model trains A, B, and C.

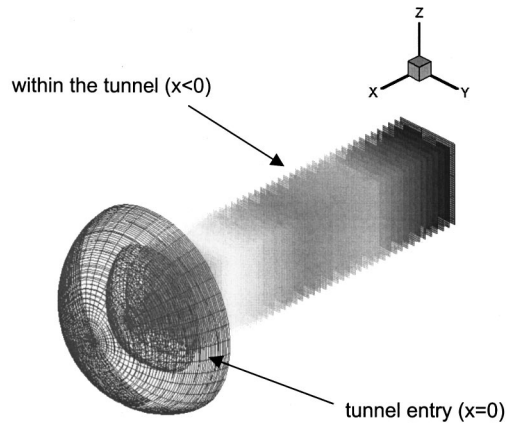

FIG. 6. Distribution of the potential function $\phi^*(\mathbf{x})$ within the tunnel and outside the tunnel.

ing the coefficient, the absorption of the acoustic wave by the ground is calculated. In the present study, the rise time of the compression wave is regarded as the characteristic time, and the absorption coefficient is determined with respect to this time. Figure 3 shows the schematics of the image source and the Kirchhoff surface under consideration. At the tunnel exit portal, the baffle plate is not installed.

V. RESULTS

A. Formation of the compression wave

All model trains have a dimension of 20 mm in diameter and a length of 2340 mm. They are used to verify two different prediction methods. One is acoustic monopole analysis and the other is CFD.

The tunnel has a rectangular shape of constant height (40 mm) and width (97 mm), corresponding to a blockage ratio of 8.1% except model A.[14] Cross-sectional areas of each tunnel and train model with its blockage ratio are listed in Table II. The track structure has the property of a ballasted track.

The blockage ratio used in prediction and experiment is very small compared to those in Japan or France. The prediction model is based upon the standards of K-HST ("Korea-High Speed Train") that will go into service in 2004. The tunnel length is 7640 mm. Figures 4(a) and (b) present the nose geometry and sketches of the three models: trains A, B, and C. Model train C is the most slender in shape. Corresponding strengths of sources (dA/dx) are plotted in Fig. 5.

The potential function distribution by Eqs. (9)–(11) is shown in Fig. 6. In the region $x>0$, namely outside the tunnel, the flow spreads hemispherically. The function $\phi^*(x)$ varies continuously through the tunnel entrance, increasing from negative values at $x<0$. In this calculation, as mentioned in Sec. II, the value of μ_a and μ_b are determined to minimize the length of end-correction by Kelvin's minimum energy principle.[5] For height (a) 40 mm and width (b) 97 mm, μ_a is 0.911 and μ_b is 0.820, respectively, and the minimized end-correction length (l') is 1.008.

At a speed of 350 km/hr (M=0.28), the entry compression wave and its pressure gradients for the three models A, B, and C are predicted by the analytic theory of Eq. (8), the result of which is plotted against nondimensional time $U[t]/a$ in Fig. 7. As shown in Table II, the blockage ratio of the model train A is slightly larger, about 0.4%, than that of model trains B and C. However, in the prediction of the compression wave, the same blockage ratio was used to investigate the effect of the train nose shape. As all the models have the same blockage ratio (8.1%), the maximum pressure rise is also the same. As for the gradient of the compression wave, however, model C has the minimum gradient. Although models A and B have the same profile nose length (l_p), the gradient of the compression wave of model B, which is relatively more blunt, is greater than that of model A. Since the magnitude of the micro-pressure wave is proportional to the pressure gradient of the compression wave arriving at the tunnel exit,[1] model B is to exhibit the micro-pressure wave of the largest amplitude.

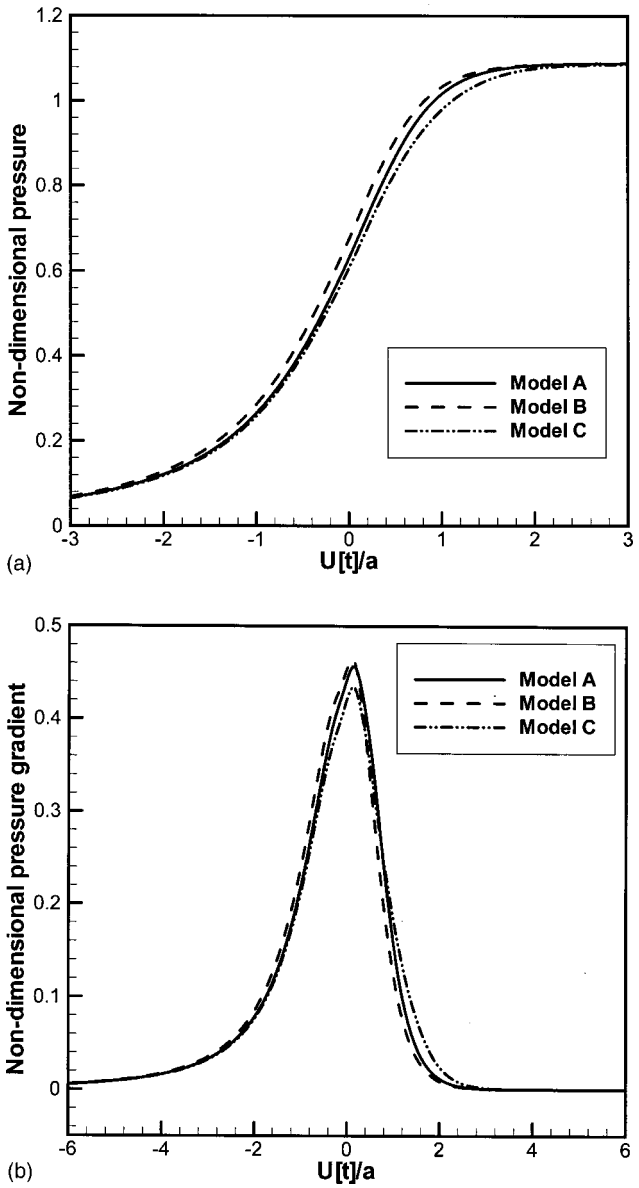

FIG. 7. (a) Entry compression wave and (b) pressure gradient for model trains A, B, and C at Mach number of 0.28 for the same blockage ratio of 8.1%. (Pressure and pressure gradient are normalized by $\rho_0 U^2 A_0/A$ and $\rho_0 U^3 A_0/aA$, respectively.)

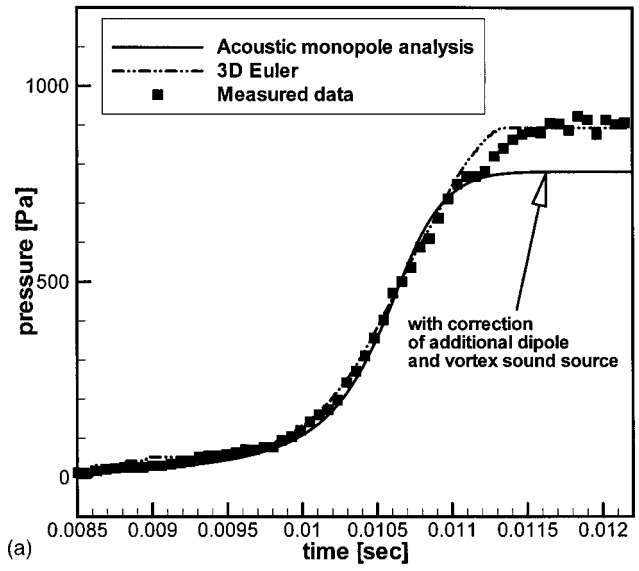

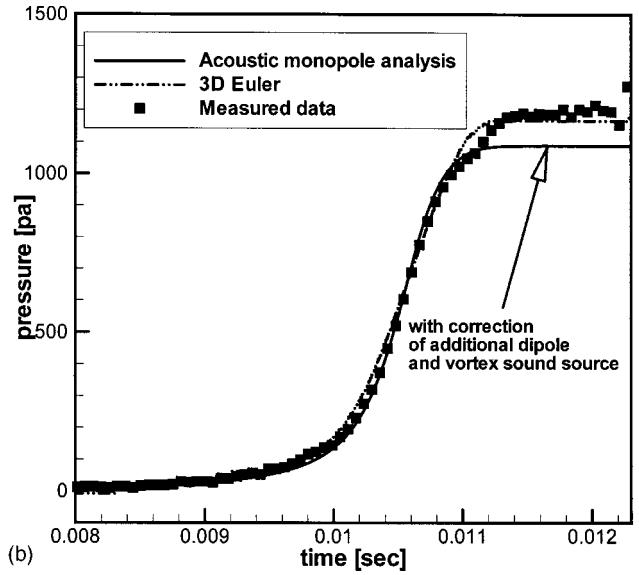

FIG. 8. Comparison with measured and predicted entry compression waves obtained by acoustic monopole analysis with second-order dipole correction and an Euler calculation for (a) 300 km/hr and (b) 350 km/hr.

To validate the prediction method, the entry compression waves at position 4.3% ($x_p/L=4.3\%$) of whole tunnel length (7640 mm) from the tunnel entry obtained by analytical theory and direct Euler computation are compared with the experimental data in Figs. 8(a) and (b). Model C is presented as a representative case. The train speed is (a) 300 km/hr and (b) 350 km/hr. Corrections to the monopole theory can be invoked to render theoretical predictions compatible with experiment.[27] First, an additional dipole source representing the compression wave drag acting on the nose of the train can be considered. The effect of this is to increase the amplitude predicted by the monopole source by a factor of $(1+A/A_0)$, where A/A_0 is the cross-sectional ratio of train to tunnel. Second, a dipole source is attributed to vortex sound sources in the shear layer of the back-flow out of the tunnel displaced by the train. This gives a progressive increase of about 1%. The measured[14] and predicted results show good agreement with each other. The prediction result

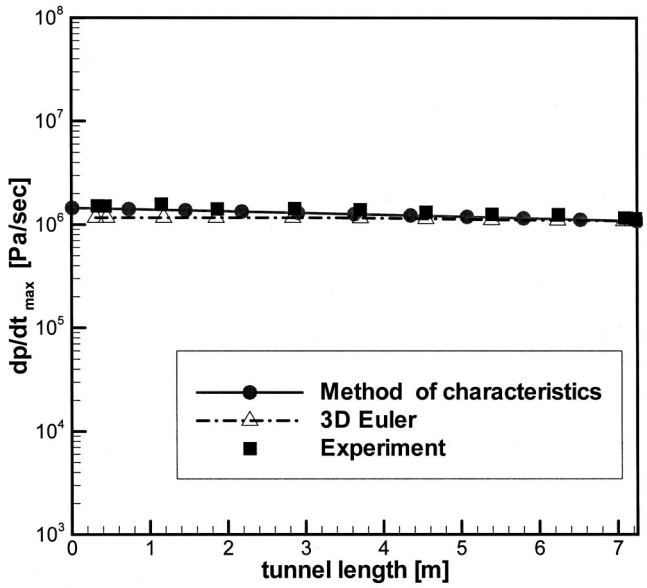

FIG. 9. Comparison with the maximum pressure gradient in the tunnel for model train C at a speed of 350 km/hr.

of the acoustic monopole with the correction of additional dipole and vortex sound source differs slightly in the maximum amplitude of pressure wave with the measured data but the gradient of the compression wave, playing an important role in generating the micro-pressure wave, approximately corresponds to the measured data. An accurate prediction of the compression wave is very important in the prediction of the micro-pressure wave because its strength is proportional to the gradient of the compression wave. In the viewpoint of computing time, the acoustic monopole method can markedly reduce the time consumption compared with the Euler simulation.

B. Propagation of the compression wave

The entry compression wave obtained by acoustic monopole analysis is used as an input to the method of characteristics. The magnitude of maximum pressure gradient in the tunnel by the method of characteristics is compared to experimental data in Fig. 9 in the case of train speed 350 km/hr for model C. The model tunnel having a length of 7640 mm is equivalent to a 1.2-km short tunnel in actual scale. Therefore, the influence of ballasted track on dissipation and dispersion of propagating compression wave is not so evident. Thus, for the prediction of propagation using the Euler equation, the track effect is not considered. It is also troublesome to consider the damping effect in the Euler equation. For a more accurate calculation, it is necessary to use a Navier–stokes solver with porous modeling on the track. As mentioned previously in Sec. I, it is appropriate to use the Euler equation in the prediction of train/tunnel aerodynamic interaction for a short tunnel because the damping effect can be regarded as negligible.

The propagation of the compression wave along the tunnel is simulated by three-dimensional Euler equation as shown in Figs. 10(a)–(d) for model train C with an entrance speed of 350 km/hr. In Fig. 10(a), it is observed that the

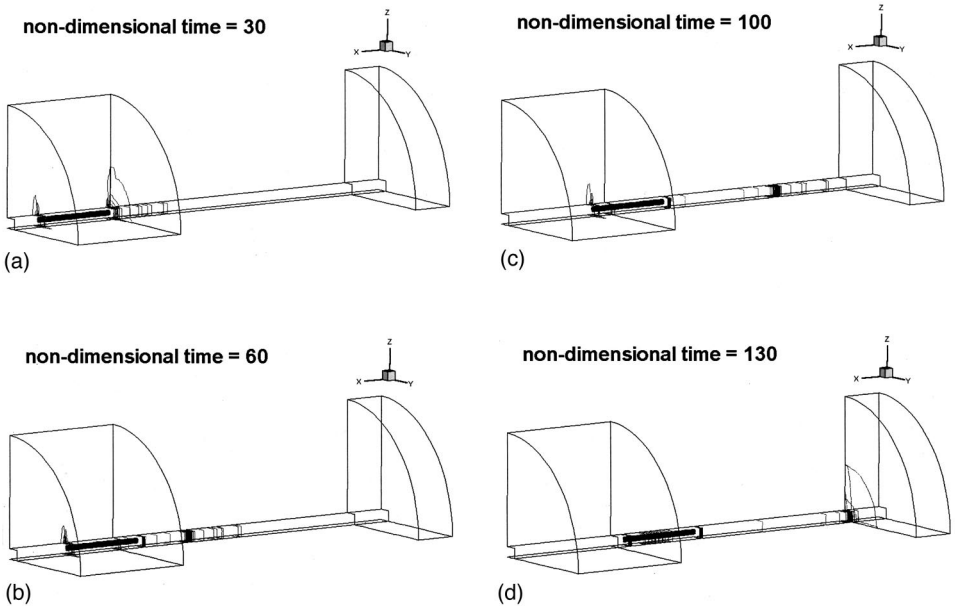

FIG. 10. Time series of the pressure contour representing the propagation of the compression wave in the case of model C having a speed of 350 km/hr.

compression wave is generated from the head of the train entering the tunnel. The compression wave propagates towards the exit of the tunnel faster than the train itself at about the speed of sound: Figs. 10(b) and (c). Finally, in Fig. 10(d), the compression wave radiates from the exit as a pulselike wave called the micro-pressure wave. Additionally the expansion wave is created at the entrance when the rear end of the train arrives at the entry of the tunnel. The predicted pressure fluctuation in the tunnel obtained by the three-dimensional Euler equation is compared with the measured data in the vicinity of the tunnel exit in Fig. 11. The measurement position is at $x_p/L=94.6\%$ from the tunnel entry. The predicted compression wave shows good agreement with the experimental data in both waveform and pressure gradient. The maximum pressure gradients in the tunnel obtained by the three-dimensional Euler equation are shown in Fig. 9. The result shows that the maximum value of pressure

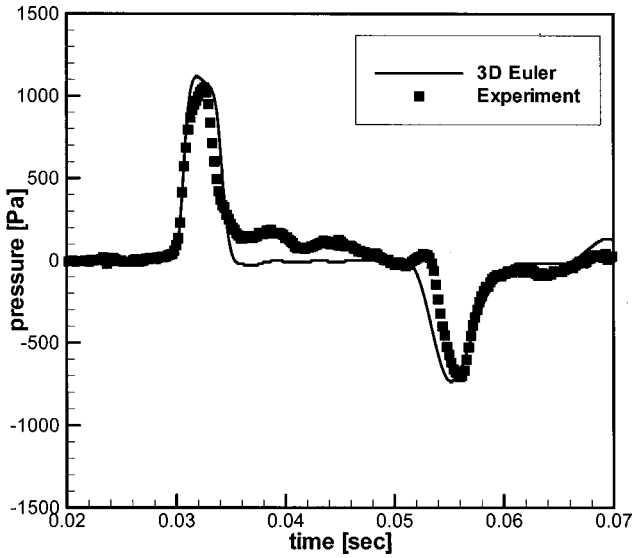

FIG. 11. Comparison of measured and predicted pressure fluctuations in the vicinity of the tunnel exit ($x_p/L=94.1\%$) obtained by 3D Euler equation for model train C at speed of 350 km/hr.

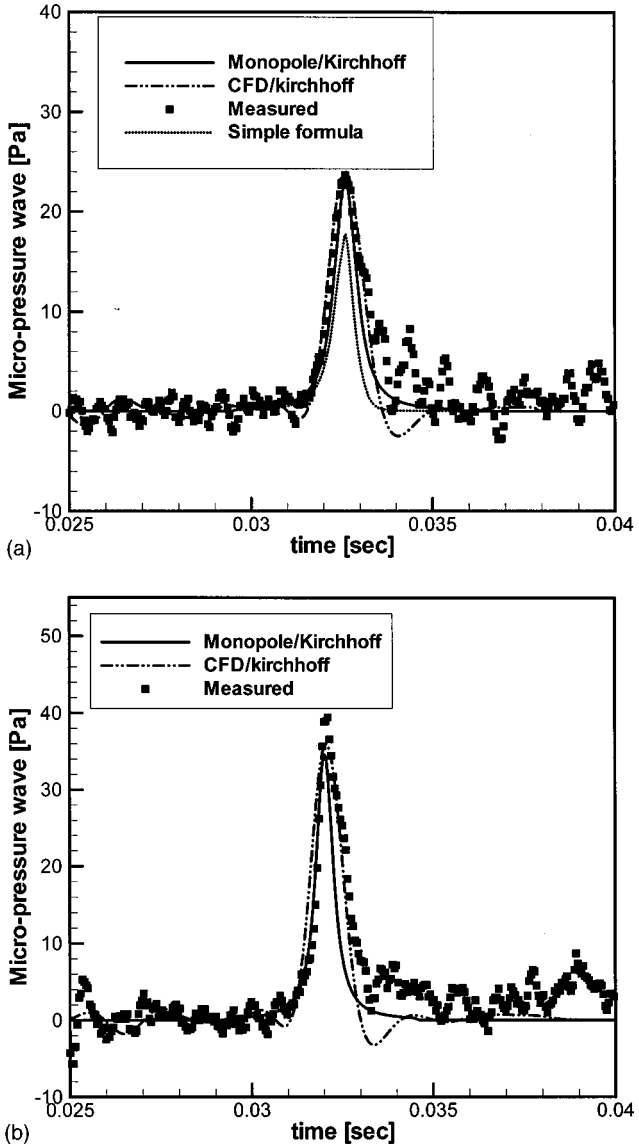

FIG. 12. Comparison of predicted and measured micro-pressure waves for (a) 300 km/hr and (b) 350 km/hr in the case of model C.

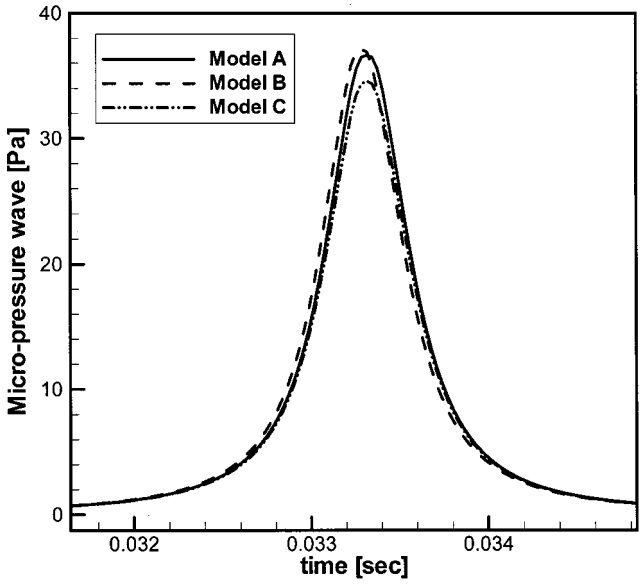

FIG. 13. Effect of the nose shape of the train on the micro-pressure wave at a speed of 350 km/hr and blockage ratio 0.081, obtained by prediction using combined acoustic monopole analysis/method of characteristics–Kirchhoff formulation.

gradient at exit (dp/dt_{EXIT}) is nearly equal to that of entry (dp/dt_{ENTRY}). Even though the experimental result shows dissipation during propagation, there is no large dissipation as can be observed in a long tunnel with ballasted track. The damping effect can thus be regarded as negligible due to the property of the short model tunnel in the Euler calculation.

C. Generation of the micro-pressure wave

The flow-field data obtained by the acoustic monopole analysis/method of characteristics and CFD is transferred to a linear Kirchhoff formulation to predict the micro-pressure wave at the exit of tunnel. Figure 12 shows the comparison of calculated results with experimental data at speeds of 300 and 350 km/hr for model train C. The micro-pressure wave is measured and predicted at 120 mm from the exit and 20 mm above the ground, inclined 45 degrees to the tunnel. For a combined acoustic monopole analysis/method of characteristics–Kirchhoff formulation, a second-order dipole correction to the monopole theory is applied as shown in Figs. 8(a) and (b). The predicted micro-pressure wave shows satisfactory agreement in both amplitude and waveform. Therefore, the proposed prediction method, a combined acoustic monopole analysis/method of characteristics–Kirchhoff method and CFD–Kirchhoff method, works very well in predicting the micro-pressure wave as well as the aerodynamic interaction between the train and the tunnel.

In previous research,[1] the following simple relationship between the micro-pressure wave and the compression wave arriving at the exit portal using far field and low-frequency approximations were used:

$$p'(\mathbf{x},t) \sim \frac{A}{\Omega a_\infty r}\left[\frac{\partial p}{\partial t}\right]_{\mathrm{EXIT},t-r/c}, \tag{16}$$

where Ω is the effective solid angle into which the wave radiates; r is the distance from the exit portal to the measured point. The dotted line in Fig. 12(a) represents the prediction result from this simple formula. In prediction by the simple formula, the pressure gradient at the tunnel exit is obtained by the acoustic monopole analysis and method of characteristics. The image source is also used to consider the ground effect as in the Kirchhoff formulation. Equation (16) underpredicts the magnitude of the micro-pressure wave by about 30%.

To obtain the entry compression waveform and the resultant micro-pressure wave, it takes 67.2×10^3 s for a combined CFD–Kirchhoff calculation, whereas a combined acoustic monopole analysis/method of characteristics–Kirchhoff requires 1.61×10^3 s. Therefore, from the engineering aspect, the combined acoustic monopole analysis/method of characteristics–Kirchhoff formulation is a very useful tool in preliminary design.

Based upon the prediction results of Figs. 7(a) and (b), the effect of nose shape of the train on the micro-pressure wave is shown in Fig. 13 for the three models with the same blockage ratio of 8.1%, using a combined acoustic monopole analysis/method of characteristics–Kirchhoff formulation. The model train C with the most slender nose generates the micro-pressure wave of the smallest magnitude.

VI. CONCLUDING REMARKS

Novel methods (combined acoustic monopole analysis/method of characteristics–Kirchhoff method, combined CFD–Kirchhoff method) were used to predict, the compression wave, the propagation of the wave in the tunnel, and the micro-pressure wave generated by a high-speed train. The near field flow data were obtained by acoustic monopole analysis/method of characteristics where the train is modeled by monopole sources and by three-dimensional Euler equations. For the monopole theory, second-order dipole corrections to the analytic theory were applied to render the prediction compatible with experimentally measured data. The flow data at the tunnel exit were transferred to the linear Kirchhoff formulation to predict the acoustic far field. The results, such as the entry compression wave, the pressure fluctuation in the tunnel, and the micro-pressure wave at exit, were compared with the measured data. The agreement was found to be good for both compression wave and micro-pressure wave.

The prediction methods can take into account the effect of nose shape of the train and the tunnel geometry. The control of nose shape can be an effective countermeasure to reduce the pressure fluctuation in the tunnel and the resulting micro-pressure wave. The study can be a very useful design tool in minimizing the pressure fluctuation and the booming noise. From the engineering viewpoint, the combined acoustic monopole/method of characteristics–Kirchhoff method is very efficient in that less computation time is involved. The method also provides the means of treating a long tunnel with concrete slab or ballasted tracks.

ACKNOWLEDGMENT

This work was supported by the Brain Korea 21 Project in 2001. The authors also appreciate the financial support from the government of Korea. This is a partial result of ''Aerodynamic Design and Analysis of High-Speed Railway System.''

[1] S. Ozawa, ''Studies of Micro-pressure Wave Radiated from a Tunnel Exit,'' Report of Railway Technical Research Institute, No. 1121 (1979) (in Japanese).
[2] M. Iida, T. Matsumura, K. Nakatani, T. Fukuda, and T. Maeda, ''Optimum Nose Shape for Reducing Tunnel Sonic Boom,'' ImechE paper C514/015/96 (1996).
[3] T. Maeda, T. Matsumura, M. Iida, K. Nakatani, and K. Uchida, K, ''Effect of shape train nose on compression wave generated by train entering tunnel'' in Proceedings of International Conference on Speedup Technology for Railway and Maglev Vehicles, Yokohama, Japan, 22–26 November 1993, pp. 315–319.
[4] M. S. Howe, ''Mach Number Dependence of the Compression wave generated by a High-Speed Train Entering a Tunnel,'' J. Sound Vib. **212**, 23–36 (1998).
[5] M. S. Howe, ''On Rayleigh's Computation of the 'end-correction', with an Application to the Compression Wave Generated by a Train Entering a Tunnel,'' J. Fluid Mech. **385**, 63–78 (1999).
[6] M. S. Howe, ''On the Compression Wave Generated when a High-Speed Train enters a Tunnel with a Flared Portal,'' J. Fluids Struct. **13**, 481–498 (1999).
[7] M. Iida, T. Matumura, K. Nakatani, T. Fukuda, and T. Maeda, ''Effective Nose Shape for Reducing Tunnel Sonic Boom,'' Quarter Report of Railway Technical Research Institute Vol. 38, No. 4 (1997) (in Japanese).
[8] T. Maeda, T. Matsumura, M. Iida, K. Nakatani, and K. Uchida, ''Effect of Shape of Train Nose on Compression Wave Generated by Train Entering Tunnel,'' in Proceedings of the International Conference on Speedup Technology for Railway and Maglev Vehicles, Yokohama, Japan (1993), pp. 315–319.
[9] T. Ogawa and K. Fujii, ''Numerical Simulation of Compressible Flows induced by a Train Moving into a Tunnel,'' Comput. Fluid Dynam. J. **3**, 63–82 (1994).
[10] T. Fukuda, M. Iida, K. Maeno, and H. Honma, ''Distortion of Compression Wave Propagating Through Slab Track Tunnel with Short Side Branches of Shinkansen,'' Proceedings of the 22nd International Symposium on Shock Waves, Imperial College, London, UK (1999), Paper 3040, pp. 1–6.
[11] T. Aoki, S. Nakano, K. Matuo, H. Kashimura, and T. Yasunobu, ''Attenuation and Distortion of Compression Wave and Shock Waves Propagating along High Speed Railway Model Tunnels,'' in Proceedings of the 21st International Symposium on Shock waves, Great Keppel Island, Australia (1997), Paper 1140, pp. 1–6.
[12] S. Ozawa, T. Uchida, and T. Maeda, ''Reduction of Micro-pressure Wave Radiated from Tunnel Exit by Hood at Tunnel Entrance,'' Quarter Report of Railway Technical Research Institute, Vol. 19, No. 2, pp. 77–83 (1978).
[13] S. Ozawa, T. Maeda, T. Matsumura, K. Uchida, H. Kajiyama, and K. Kanemoto, ''Countermeasures to Reduce Micro-pressure Waves Radiating from Exits of Shinkansen Tunnels,'' in *Aerodynamics and Ventilation of Vehicle Tunnels* (Elsevier Science, Oxford, 1991), pp. 253–266.
[14] T. Yoon, S. Lee, J. Hwang, and D. Lee, ''Prediction and Validation on the Sonic Boom by a High Speed Train Entering a Tunnel,'' J. Sound Vib. **247**, 195–211 (2001).
[15] S. Ozawa, T. Maeda, T. Matsumura, and K. Uchida, ''Effect of Ballast on Pressure Wave Propagating through Tunnel—1st Report; Investigation of Actual Conditions and Formulation of Basic Equations by One-dimensional Model,'' Report of Railway Technical Research Institute, Vol. 5, No. 12, pp. 9–15 (1991) (in Japanese).
[16] P. L. Roe, ''Approximate Riemann Solvers, Parameter Vectors and Difference Schemes,'' J. Comput. Phys. **43**, 357–372 (1981).
[17] A. Jameson and S. Yoon, ''Lower-Upper Implicit Schemes with Multiple Grids for the Euler Equations,'' AIAA J. **25**, 929–935 (1987).
[18] K. Fujii, ''Unified Zonal Method Based on the Fortified Solution Algorithm,'' ISAS Report No. 648, December (1992).
[19] E. Mestreau, R. Lohner, and S. Aita, ''TGV Tunnel Entry Simulations Using a Finite Element Code with Automatic Remeshing,'' AIAA Pap., 93–0890 (1993).
[20] J. L. Steger, F. C. Dougherty, and J. A. Benek, ''A Chimera Grid Scheme,'' in *Advances in Grid Generation, FED Vol. 5*, edited by K. N. Ghia (ASME, New York, 1983), pp. 59–69.
[21] M. M. Rai and K. Hessenius, ''Three Dimensional Conservative Euler Computations Using Patched Grid System and Explicit Methods,'' AIAA Pap., 86–1081 (1986).
[22] B. B. Bakerand and E. T. Copson, *The Mathematical Theory of Huygens' Principle* (Clarendon, Oxford, 1953).
[23] A. S. Lyrintzis, ''Review: The Use of Kirchhoff's Method in Computational Aeroacoustics,'' ASME J. Fluids Eng. **116**, 665–676 (1994).
[24] S. Lee, J. Kim, Y. H. Yu, and M. P. Isom, ''Prediction of Rotor High-Speed Impulsive Noise with a Combined CFD-Kirchhoff Method,'' J. Sound Vib. **207**(4), 453–464 (1997).
[25] Y. Xue and A. S. Lyrintzis, ''The Use of Rotating Kirchhoff formulation for 3-d Transonic BVI Far-field Noise,'' in 49th Annual Forum of the America Helicopter Society, St. Louis, MO (1993).
[26] C. M. Harris, *Handbook of Acoustical Measurements and Noise Control* (McGraw–Hill, New York, 1991).
[27] M. S. Howe, M. Iida, T. Fukuda, and T. Maeda, ''Theoretical and Experimental Investigation of the Compression Wave Generated by a Train Entering a Tunnel with a Flared Portal,'' J. Fluid Mech. **425**, 111–132 (2000).